# Optimal Persistent Currents for Interacting Bosons on a Ring with a Gauge Field

Marco Cominotti,[1,2] Davide Rossini,[3] Matteo Rizzi,[4] Frank Hekking,[1,2] and Anna Minguzzi[1,2]
[1]*Université Grenoble Alpes, LPMMC, F-38000 Grenoble, France*
[2]*CNRS, LPMMC, F-38000 Grenoble, France*
[3]*NEST, Scuola Normale Superiore and Istituto Nanoscienze-CNR, I-56126 Pisa, Italy*
[4]*Institut für Physik, Johannes-Gutenberg-Universität Mainz, Staudingerweg 7, D-55099 Mainz, Germany*
(Received 1 October 2013; published 7 July 2014)

We study persistent currents for interacting one-dimensional bosons on a tight ring trap, subjected to a rotating barrier potential, which induces an artificial $U(1)$ gauge field. We show that, at intermediate interactions, the persistent current response is maximal, due to a subtle interplay of effects due to the barrier, the interaction, and quantum fluctuations. These results are relevant for ongoing experiments with ultracold atomic gases on mesoscopic rings.

DOI: 10.1103/PhysRevLett.113.025301 PACS numbers: 67.85.−d, 03.75.Lm, 05.60.Gg, 71.10.Pm

A quantum fluid confined on a ring and subjected to a $U(1)$ gauge potential displays a periodicity in the particle current as a function of the flux of the corresponding classical gauge field. This persistent current phenomenon is a manifestation of the Aharonov-Bohm effect and reflects the macroscopic coherence of the many-body wave function along the ring. Such currents were observed more than 50 years ago in bulk superconductors [1] and, more recently, in normal metallic rings, overcoming the challenges of the decoherence induced by inelastic scattering [2]. The most recent developments in the manipulation of ultracold atoms on ring traps [3,4] have disclosed a novel platform for the study of persistent currents, which can be induced by the application of a rotating localized barrier or, alternatively, by inducing suitable artificial gauge fields [5]. Tunable localized barriers in toroidal Bose-Einstein condensates have been realized, using well-focused, repulsively tuned laser beams [4]. Also, recently the engineering of an atomic superconducting quantum interference device was demonstrated [6]. The unprecedented variety of interaction and barrier strength regimes paves the way to applications such as high-precision measurements, atom interferometry, and quantum information, e.g., by the construction of macroscopic superposition of current states and flux qubits [7–9].

The scenario becomes particularly intriguing if the transverse section of the ring is sufficiently thin to effectively confine the system in one dimension (1D): the rich interplay between interactions, quantum fluctuations, and statistics acquires a role of primary relevance. In absence of any obstacle along the ring, the persistent currents display an ideal sawtooth behavior as a function of the flux, i.e., perfect superfluidity for any interaction strength at zero temperature [10,11]. Diamagnetic or paramagnetic response depending on the population parity is expected [12] for fermions but not for bosons. If a localized barrier is added, persistent currents are smeared—their shape taking a sinusoidal form in the case of large-barrier or small-tunneling limit—as obtained for thin superconducting rings from a Luttinger-liquid approach [13]. Beyond these limiting regimes, the physics of bosonic persistent current remains unexplored.

The aim of the present work is to provide a complete characterization of persistent currents for 1D bosons, in all interaction and barrier strength regimes. By combining analytical as well as numerical techniques suited for the 1D problem, we show that the current amplitude is a nonmonotonic function of the interaction strength and displays a pronounced maximum in all regimes of barrier height. The presence of an optimal regime illustrates the highly nontrivial combination of correlations, quantum fluctuations, and barrier effects. Our results demonstrate that, in a large range of interaction strengths, unwanted impurities or imperfections on the ring only weakly affect the system properties. For the application to quantum state manipulation, the regimes of choice should be either very weak or very strong interactions, where the response to a localized external probe is stronger. Our predictions are readily amenable to experimental testing with quasi-1D ultracold atomic gases confined in mesoscopic uniform and lattice rings. Indeed, all the interaction regimes, from weakly interacting quasicondensate to the impenetrable-boson Tonks-Girardeau limit, have been experimentally demonstrated for 1D bosonic wires [14].

*Persistent currents for bosons under a gauge field.*—Let us consider a 1D ring of circumference $L$, containing $N$ bosons of mass $M$ interacting with each other via a contact potential $v(x-x') = g\delta(x-x')$. The ring contains a localized barrier modeled as $U_b(x,t) = U_0\delta(x-Vt)$, moving along its circumference at constant velocity $V$. This induces an effective gauge field with Coriolis flux $\Omega = MVL/2\pi\hbar$ in the rotating frame. In the corotating frame, the Hamiltonian reads

$$\mathcal{H} = \sum_{j=1}^{N} \frac{\hbar^2}{2M}\left(-i\frac{\partial}{\partial x_j} - \frac{2\pi}{L}\Omega\right)^2 + U_0\delta(x_j) + \frac{g}{2}\sum_{j,l=1}^{N}\delta(x_l - x_j). \quad (1)$$

 

This generalizes the Lieb-Liniger model [15] to the rotating case and is nonintegrable due to the presence of the barrier. The corresponding many-body energy spectrum is periodic in $\Omega$ with period 1, giving rise to the Aharanov-Bohm effect.

We consider the stationary regime, reached after the barrier has been adiabatically switched on at early times, such that no high-energy excitations are created. At zero temperature, the spatially averaged particle current $I(\Omega)$, or persistent current, is obtained from the ground-state energy $E(\Omega)$ via the thermodynamic relation [16]

$$I(\Omega) = -\frac{1}{2\pi\hbar}\frac{\partial E(\Omega)}{\partial \Omega}. \quad (2)$$

In absence of a barrier, for any interaction strength, the ground-state energy is given by a series of parabolas with well-defined angular momentum, shifted with respect to each other by Galilean translation [17] and intersecting at the frustration points $\Omega_j = (2j+1)/2$. The corresponding persistent current (Fig. 1) is a perfect sawtooth in the rotating frame and a staircase in the nonrotating frame, corresponding to states with well-defined angular momentum (dashed lines). The addition of a barrier breaks the rotational invariance and induces coherent superpositions of states of different angular momentum. This gives rise to gap openings in the many-body energy spectrum at the frustration points, thus forming the working points for a qubit based on a superposition of current states. The level mixing is visible in the persistent current. In the rotating frame, $I(\Omega)$ is a smeared sawtooth for weak barriers (solid lines) and a sinusoid for large barriers (dotted lines). In order to characterize the qubit, we focus on the amplitude $\alpha$ of the persistent current in the rotating frame, determining its value for all regimes of dimensionless interaction strength $\gamma = Mg/\hbar^2 n_0$, with $n_0 = N/L$, and dimensionless barrier height $\lambda = MU_0 L/\pi\hbar^2$.

*Noninteracting and impenetrable boson limits.*—Both for zero and infinitely large repulsive interactions, it is possible to find an exact solution to the many-body Schrödinger equation $\mathcal{H}\Psi(x_1,\ldots,x_N) = E\Psi(x_1,\ldots,x_N)$. For a noninteracting (NI) Bose gas, the many-body wave function $\Psi_{\rm NI}(x_1,\ldots,x_N) = \prod_{i=1}^{N}\psi_0(x_i)$ is simply given by the product of $N$ identical single-particle wave functions $\psi_0(x_i)$, which are ground-state solutions of the corresponding one-body Schrödinger equation, $(\hbar^2/2M)[-i\partial_x - (2\pi/L)\Omega]^2\psi_n + U_0\delta(x)\psi_n = \varepsilon_n\psi_n$, and has energy $E_{\rm NI} = N\varepsilon_0$. In the infinitely interacting limit of impenetrable bosons, or Tonks-Girardeau (TG) gas, the solution is obtained by mapping the system onto a gas of noninteracting fermions subjected to the same external potential [18], $\Psi_{\rm TG}(x_1,\ldots,x_N) = \prod_{1\le j<\ell\le N}\mathrm{sgn}(x_j - x_\ell)\times\det[\psi_k(x_i)]$. The corresponding energy $E_{\rm TG} = \sum_{k=0}^{N-1}\varepsilon_k$ and density profile $n(x) = \sum_{k=0}^{N-1}|\psi_k|^2$ directly reflect the fermionization properties of the strongly interacting Bose gas. The Friedel oscillations of the density profile [Fig. 2(d)] are indeed a signature of the strongly correlated regime [19].

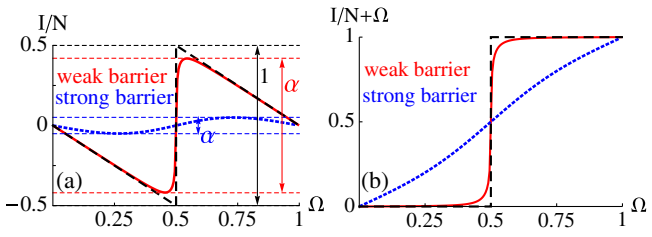


FIG. 1 (color online). Persistent current (a) in the rotating frame and (b) in the nonrotating frame, in units of $I_0 = 2\pi\hbar/ML^2$ for $N = 18$, for zero barrier (black dashed line), weak barrier ($\lambda = 0.2$, red solid line), and strong barrier ($\lambda = 10$, blue dotted line) at fixed interaction strength ($\gamma = 0.004$).

The persistent current amplitude in the zero and infinitely interacting limits, obtained from Eq. (2) (see the Supplemental Material [21]), is shown in Fig. 3. We find that the current amplitude depends on the interaction regime. In particular, for all values of barrier strength, $\alpha$ is always larger in the strongly interacting regime than in the noninteracting one. This behavior is explained by noticing that the barrier affects the lowest-lying energy levels more than the high-energy ones [8]. As a result, the current amplitude is smaller for noninteracting bosons, occupying only the lowest level, than for the TG gas, where the levels are filled up to the Fermi energy.

*Weak interactions.*—In order to explore the role of interactions for quantum state manipulation, we start from the noninteracting result and consider the effect of weakly repulsive interactions. In this regime, we neglect quantum fluctuations [29] and describe the fluid as a Bose-Einstein condensate, making use of the mean-field Gross-Pitaevskii (GP) equation. In the corotating frame, this takes the form $(\hbar^2/2M)[-i\partial_x - (2\pi/L)\Omega]^2\Phi + U_0\delta(x)\Phi + g|\Phi|^2\Phi = \mu\Phi$, where $\Phi$ is the condensate wave function and $\mu$ is the chemical potential. This equation admits stable dark-soliton solutions, with a size given by the healing length $\xi = \hbar/\sqrt{2Mgn_0}$. We have found an analytical solution for $\Phi$ in terms of Jacobi elliptic functions (Supplemental Material [21]), thus extending Refs. [30] (see also Ref. [31]). In particular, by comparing it with the numerical solution of the GP equation, we find that the barrier pins the soliton and turns it to the ground-state solution. The resulting density profile has a minimum at the barrier position. The depth and the healing length of the soliton depend on the interaction strength, the barrier height, and the rotation velocity [see Fig. 2(a) and the Supplemental Material [21] ]. The solitary suppression of the density is accompanied by a winding of the superfluid phase, known as a phase slip [inset of Fig. 2 (a)]. We note that a finite-width barrier, as could be realized experimentally, yields very similar profiles [Fig. 2(b)]. Its extension to multiple finite-width barriers is known to give rise to a wealth of nonlinear modes [32].

The soliton energy is obtained from the GP energy functional $E_{\rm GP}[\Phi] = \int dx\Phi^*(\hbar^2/2M)[-i\partial_x - (2\pi/L)\Omega]^2\Phi + g|\Phi|^4/2 + U_0\delta(x)|\Phi|^2$, which encodes the dependence on $\Omega$ also in the condensate wave function. Computing the persistent current amplitude $\alpha$, we find that it increases

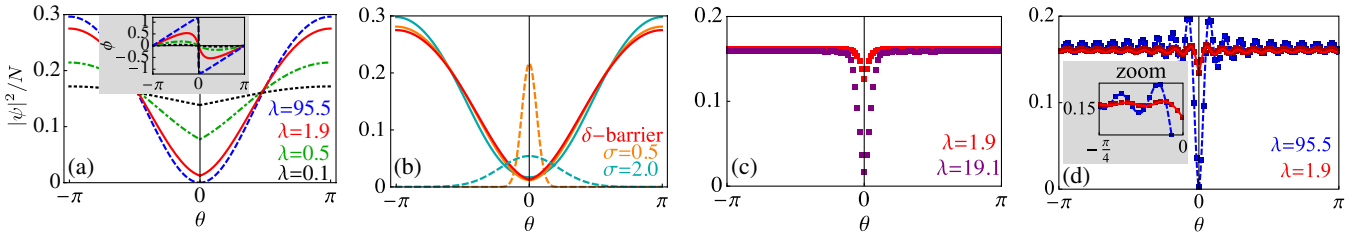


FIG. 2 (color online). Density profiles vs angular coordinate $\theta$ along the ring. (a) GP analytical solution at weak interaction strength $\gamma = 0.01$ for a delta barrier for various values of the barrier strength $\lambda$; the inset shows the soliton phase vs $\theta$ for the same values of barrier strength. (b) GP numerical solution (solid lines) at $\gamma = 0.01$ for a Gaussian barrier of strength $\lambda = 1.9$ for various values of the barrier width $\sigma$ (in units of $n_0^{-1}$) and corresponding barrier potential (dashed lines, in units of $10 \times 2\pi^2\hbar^2/mL^2$). (c) MPS solution at intermediate interaction $\gamma = 3.3$ and filling 0.15. (d) Analytical TG solution (lines) vs MPS (squares) in the hard-core limit. The other parameters used are $N = 18$ and $\Omega = 0.4$ in all the curves.

monotonically with the interaction strength $\gamma$, as illustrated in Fig. 3. This is due to the fact that the healing length $\xi$ decreases at increasing interaction strength, thus yielding a more effective screening of the barrier, thereby restoring superfluidity.

*Strong interactions.*—We now turn to the effect of quantum fluctuations on the persistent current at strong interparticle interactions, up to the TG limit. This can be achieved with the help of Luttinger liquid (LL) theory [33], a low-energy, quantum hydrodynamics description of the bosonic fluid, in terms of the canonically conjugate fields $\theta$ and $\phi$ corresponding to density fluctuations and superfluid phase, respectively. In the rotating frame, the effective LL Hamiltonian for a uniform ring is

$$\mathcal{H}_0 = \frac{\hbar v_s}{2\pi}\int_0^L dx\left[K\left(\partial_x\phi(x) - \frac{2\pi}{L}\Omega\right)^2 + \frac{1}{K}(\partial_x\theta(x))^2\right]. \tag{3}$$

The microscopic interaction strength enters through the Luttinger parameter $K$ and the sound velocity $v_s$. In the case

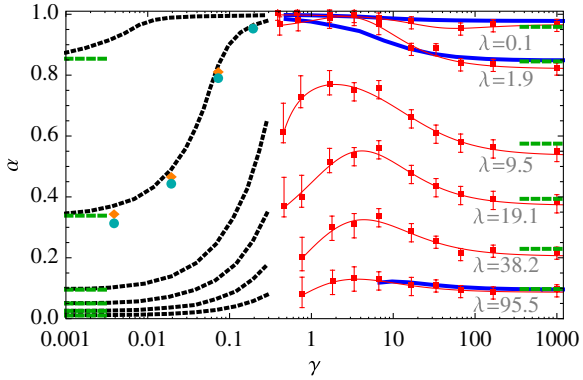


FIG. 3 (color online). Persistent current amplitude $\alpha$, in units of $I_0 = 2\pi\hbar/ML^2$, as a function of the interaction strength $\gamma$ at varying barrier strength $\lambda$, for $N = 18$, from GP equation (black dotted lines), LL approach (blue solid lines), numerical MPS calculations (red squares, with red thin lines as guides to the eye), and NI and TG exact solutions (green dashes). Orange diamonds and cyan circles are for a Gaussian barrier of width $\sigma = 0.5, 2(n_0^{-1})$, respectively.

of repulsive contact interactions, their dependence on the interaction strength is known (see, e.g., Ref. [34]): at vanishing interactions, $K$ tends to infinity and $v_s$ vanishes, while, in the TG limit, $K = 1$ and $v_s$ corresponds to the Fermi velocity of the fermionized Bose gas.

In the presence of a barrier, nonlinear terms appear in the Hamiltonian. We treat these perturbatively in the limits of weak and strong barrier strength. In the regime of a weak barrier, its contribution to the Hamiltonian $\mathcal{H}_b = \int dx U_0\delta(x)\rho(x)$ is obtained by keeping only the lowest harmonics in the density field expansion $\rho(x) = [n_0 + \partial_x\theta(x)/\pi]\sum_{l=-\infty}^{+\infty} e^{2il\theta(x)+2il\pi n_0 x}$, yielding as the most important term $\mathcal{H}_b \sim 2U_0 n_0\cos[2\theta(0)]$. This backscattering term breaks angular momentum conservation, allowing for transitions between angular momentum states [35]. At the same time, quantum fluctuations renormalize the barrier strength down according to $U_{\rm eff} = U_0(d/L)^K$, where $d$ is a suitably chosen short-distance cutoff (see the Supplemental Material [21]). As a result, the persistent current close to the frustration point $\Omega = 1/2$ is a smeared sawtooth

$$I(\Omega)/N = -I_0\delta\Omega[1 - (\sqrt{4\delta\Omega^2 + \lambda_{\rm eff}^2/\pi^2})^{-1}], \tag{4}$$

where $\delta\Omega = \Omega - 1/2$, $\lambda_{\rm eff} = MU_{\rm eff}L/\pi\hbar^2$, and $I_0 = 2\pi\hbar/ML^2$. The corresponding amplitude $\alpha$ is shown in Fig. 3. For decreasing interactions down from the TG limit, the quantum fluctuations of density increase, suppressing the barrier more strongly, hence, increasing $\alpha$.

In the opposite case of strong barrier strength, we model the transport across the barrier with a tunneling Hamiltonian $\mathcal{H}_t = -2tn_0\cos[\phi(L) - \phi(0) + 2\pi\Omega]$, where $t$ is the tunneling amplitude. In this limit, quantum phase fluctuations lead to a renormalization down of the tunnel amplitude [36], i.e.,

$$I(\Omega)/N = -(2t/L\hbar)(d/L)^{1/K}\sin(2\pi\Omega). \tag{5}$$

Note the dual nature of this result (power $1/K$) in comparison to the one obtained above for a weak barrier (power $K$). Indeed, the quantum phase fluctuations increase with increasing interactions, thereby suppressing the tunneling amplitude more, thus, decreasing $\alpha$. The duality between the two models

can also be used to establish a link between the tunnel amplitude and the barrier height [21,38]. The persistent current amplitude for large barrier is also shown in Fig. 3. Interestingly, the renormalization by quantum fluctuations at intermediate interactions is effective enough to turn a relatively large barrier into a weak one. This quantum healing phenomenon completely changes the physical scenario and illustrates the dramatic effect of interplay of interactions and quantum fluctuations.

Both for weak and large barriers, the LL description breaks down for sufficiently weak interactions when the short-distance cutoff required in the theory increases, until it becomes comparable with the system size.

*Intermediate interactions and barrier strengths.*—Away from the weakly and the strongly interacting regime and for arbitrary barrier strength, it is difficult to tackle the many-body Schrödinger equation corresponding to the Hamiltonian of Eq. (1) with analytical approaches; therefore, we employ numerical simulations based on the density-matrix renormalization-group (see the Supplemental Material [21]). After discretizing the space on $N_s$ sites and using the standard Peierls construction, we map Eq. (1) onto a Bose-Hubbard (BH) model on a 1D ring lattice at low filling,

$$\mathcal{H}_{\rm lat} = \sum_{j=1}^{N_s} -t_{\rm BH}(e^{-(2\pi i\Omega/N_s)} b_j^\dagger b_{j+1} + \text{H.c.}) + \frac{U_{\rm BH}}{2} n_j(n_j-1) + (\beta\delta_{j,1} n_j - \mu n_j), \quad (6)$$

where $b_j^\dagger$ ($b_j$) are bosonic creation (annihilation) operators at site $j$, $t_{\rm BH}$ is the tunnel energy for bosons on adjacent sites, and $U_{\rm BH}$ is the on-site repulsion energy. The phase twist $\Omega/N_s$ accounts for the effect of the Coriolis flux, $\beta$ is the barrier strength, and $\mu$ is the chemical potential. An experimental implementation of the Hamiltonian of Eq. (6) with a localized barrier on one lattice site has been recently proposed [9]. We compute the ground-state wave function and energy using a matrix product state (MPS) [39], optimized for periodic boundary conditions (Supplemental Material [21]). The resulting density profiles are shown in Figs. 2(c) and 2(d). As compared to Fig. 2(a), the healing effect is much more pronounced and might be efficiently used to screen unwanted impurities. As anticipated above, for large interactions the density profiles display Friedel oscillations, in very good agreement with the analytical predictions in the TG limit. The oscillations are strongly damped at intermediate and weak interactions. We also compute the amplitude $\alpha$ of the persistent current for a large range of barrier heights $\lambda$ and interaction strengths $\gamma$ (Fig. 3) [40]. We find a nonmonotonic behavior connecting the weak- and strong-interaction results as a consequence of the subtle interplay between backscattering and interaction effects. This result allows us to confirm the expected regimes of validity of the analytical estimates. We note that the position of the maximum, i.e., the optimum persistent current, depends on the barrier strength.

*Experimental considerations.*—Our results are also valid for finite-width barriers, used in realistic implementations. We have checked that the use of a Gaussian barrier does not lead to qualitative changes of our results in the mean-field regime [41] (see Fig. 3 for a choice of barrier strength; similar results hold for all the barrier strength regimes), provided that the barrier width remains comparable to the interparticle distance, a condition achievable, e.g., with a microscope-focused stirring beam [43]. Thermal fluctuations give rise to additional smearing of persistent currents starting from a typical temperature $k_B T \sim NE_0 = 2\pi^2\hbar^2 n_0/ML$ [11,12,44]. Within typical experimental constraints on energy and time scales, persistent currents might be observed in the next-generation experiments of mesoscopic ring traps on a chip (i.e., with a ring diameter of $\sim 5$ $\mu$m), corresponding to a typical energy $NE_0 \sim$ 550 Hz for $^{87}$Rb atoms taking $N = 18$, as in Fig. 3.

*Conclusions.*—We disclosed the role of quantum fluctuations and correlations in the emergence of persistent currents of rotating bosons in reduced dimensionality, in the presence of a localized barrier. Our results, summarized in Fig. 3, evidence the presence of a maximum as a function of the interaction strength, which is due to the competition between correlations and fluctuations. While at increasing interactions a classical bosonic field screens the barrier more and more, going towards the strongly correlated Tonks-Girardeau regime quantum fluctuations screen the barrier less and less, due to the increasingly fast spatial decay of phase-phase correlations [45]. These predictions can be tested via time-of-flight measurements, similar to those used to probe circulation in atomic rings [3,4].

In the present work we studied a thermodynamic quantity —the persistent current—but the interplay of barrier and quantum fluctuations will have a similar impact on out-of-equilibrium properties involving wave emission, ranging from collective modes to transport phenomena, including shock wave generation and Hawking radiation of superfluids [47]. Our results are also relevant to other mesoscopic bosonic quantum fluids, as thin superconducting rings, photons in nonlinear twisted-pipe waveguides, and solid-state photonic or polaritonic nanocavities etched on a ring-necklace shape.

We are indebted to L. Amico, R. Citro, R. Fazio, L. Glazman, N. Pavloff, I. Safi, P. Silvi, and W. Zwerger for discussions. This work is supported by the ERC Handy-Q Grant No. 258608, the Institut Universitaire de France, and the Italian MIUR through FIRB Project RBFR12NLNA. MPS simulations were performed on the TQO cluster of the Max-Planck-Institut für Quantenoptik (Garching) and on the MOGON cluster in Mainz.

[1] B. S. Deaver and W. M. Fairbank, Phys. Rev. Lett. **7**, 43 (1961); N. Byers and C. N. Yang, Phys. Rev. Lett. **7**, 46 (1961); L. Onsager, Phys. Rev. Lett. **7**, 50 (1961).

[2] L. P. Lévy, G. Dolan, J. Dunsmuir, and H. Bouchiat, Phys. Rev. Lett. **64**, 2074 (1990); D. Mailly, C. Chapelier, and A. Benoit, Phys. Rev. Lett. **70**, 2020 (1993); H. Bluhm, N. C. Koshnick,

J. A. Bert, Julie M. E. Huber, and K. A. Moler, Phys. Rev. Lett. **102**, 136802 (2009); A. C. Bleszynski-Jayich, W. E. Shanks, B. Peaudecerf, E. Ginossar, F. von Oppen, L. Glazman, and J. G. E. Harris, Science **326**, 272 (2009).

[3] S. Gupta, K. W. Murch, K. L. Moore, T. P. Purdy, and D. M. Stamper-Kurn, Phys. Rev. Lett. **95**, 143201 (2005); C. Ryu, M. F. Andersen, P. Cladé, V. Natarajan, K. Helmerson, and W. D. Phillips, Phys. Rev. Lett. **99**, 260401 (2007); W. H. Heathcote, E. Nugent, B. T. Sheard, and C. J. Foot, New J. Phys. **10**, 043012 (2008); K. Henderson, C. Ryu, C. MacCormick, and M. G. Boshier, New J. Phys. **11**, 043030 (2009); B. E. Sherlock, M. Gildemeister, E. Owen, E. Nugent, and C. J. Foot, Phys. Rev. A **83**, 043408 (2011); S. Moulder, S. Beattie, R. P. Smith, N. Tammuz, and Z. Hadzibabic, Phys. Rev. A **86**, 013629 (2012); S. Beattie, S. Moulder, R. J. Fletcher, and Z. Hadzibabic, Phys. Rev. Lett. **110**, 025301 (2013).

[4] A. Ramanathan, K. C. Wright, S. R. Muniz, M. Zelan, W. T. Hill, III, C. J. Lobb, K. Helmerson, W. D. Phillips, and G. K. Campbell, Phys. Rev. Lett. **106**, 130401 (2011); K. C. Wright, R. B. Blakestad, C. J. Lobb, W. D. Phillips, and G. K. Campbell, Phys. Rev. Lett. **110**, 025302 (2013).

[5] J. Dalibard, F. Gerbier, G. Juzeliūnas, and P. Öhberg, Rev. Mod. Phys. **83**, 1523 (2011).

[6] C. Ryu, P. W. Blackburn, A. A. Blinova, and M. G. Boshier, Phys. Rev. Lett. **111**, 205301 (2013).

[7] D. W. Hallwood, T. Ernst, and J. Brand, Phys. Rev. A **82**, 063623 (2010); D. Solenov and D. Mozyrsky, Phys. Rev. A **82**, 061601 (2010); A. Nunnenkamp, A. M. Rey, and K. Burnett, Phys. Rev. A **84**, 053604 (2011); D. Solenov and D. Mozyrsky, J. Comput. Theor. Nanosci. **8**, 481 (2011).

[8] C. Schenke, A. Minguzzi, and F. W. J. Hekking, Phys. Rev. A **84**, 053636 (2011).

[9] L. Amico, D. Aghamalyan, F. Auksztol, H. Crepaz, R. Dumke, and L.-C. Kwek, Sci. Rep. **4**, 4298 (2014).

[10] A. J. Leggett, in *Granular Nanoelectronics*, edited by D. K. Ferry, J. R. Barker, and C. Jacoboni, Nato ASI Series B, Vol. 251 (Plenum, New York, 1991), p. 297; A. Mueller-Groeling, H. A. Weidenmueller, and C. H. Lewenkopf, Europhys. Lett. **22**, 193 (1993).

[11] D. Loss, Phys. Rev. Lett. **69**, 343 (1992).

[12] A. A. Zvyagin and I. V. Krive, Low Temp. Phys. **21**, 533 (1995).

[13] F. W. J. Hekking and L. I. Glazman, Phys. Rev. B **55**, 6551 (1997); K. A. Matveev, A. I. Larkin, and L. I. Glazman, Phys. Rev. Lett. **89**, 096802 (2002).

[14] S. Dettmer, D. Hellweg, P. Ryytty, J. J. Arlt, W. Ertmer, K. Sengstock, D. S. Petrov, G. V. Shlyapnikov, H. Kreutzmann, L. Santos, and M. Lewenstein, Phys. Rev. Lett. **87**, 160406 (2001); F. Gerbier, J. H. Thywissen, S. Richard, M. Hugbart, P. Bouyer, and A. Aspect, Phys. Rev. A **67**, 051602 (2003); B. Paredes, A. Widera, V. Murg, O. Mandel, S. Fölling, I. Cirac, G. V. Shlyapnikov, T. W. Hänsch, and I. Bloch, Nature (London) **429**, 277 (2004); T. Kinoshita, T. Wenger, and D. S. Weiss, Science **305**, 1125 (2004).

[15] E. H. Lieb and W. Liniger, Phys. Rev. **130**, 1605 (1963).

[16] F. Bloch, Phys. Rev. B **2**, 109 (1970).

[17] F. Bloch, Phys. Rev. A **7**, 2187 (1973).

[18] M. Girardeau, J. Math. Phys. (N.Y.) **1**, 516 (1960).

[19] The Friedel oscillations weakly depend on the rotation velocity, as in Ref. [20].

[20] W. Zwerger, L. Bönig, and K. Schönhammer, Phys. Rev. B **43**, 6434 (1991).

[21] See the Supplemental Material at http://link.aps.org/supplemental/10.1103/PhysRevLett.113.025301, which includes Refs. [22–28], for details.

[22] A. O. Gogolin and N. V. Prokof'ev, Phys. Rev. B **50**, 4921 (1994).

[23] U. Schollwöck, Ann. Phys. (Amsterdam) **326**, 96 (2011).

[24] F. Verstraete, D. Porras, and J. I. Cirac, Phys. Rev. Lett. **93**, 227205 (2004).

[25] F. Verstraete, V. Murg, and J. I. Cirac, Adv. Phys. **57**, 143 (2008).

[26] P. Pippan, S. R. White, and H. G. Evertz, Phys. Rev. B **81**, 081103(R) (2010).

[27] D. Rossini, V. Giovannetti, and R. Fazio, J. Stat. Mech. (2011) P05021.

[28] M. Weyrauch and M. V. Rakov, Ukr. Phys. J. **58**, 657 (2013).

[29] D. S. Petrov, G. V. Shlyapnikov, and J. T. M. Walraven, Phys. Rev. Lett. **85**, 3745 (2000).

[30] R. Kanamoto, L. D. Carr, and M. Ueda, Phys. Rev. Lett. **100**, 060401 (2008); R. Kanamoto, L. D. Carr, and M. Ueda, Phys. Rev. A **79**, 063616 (2009).

[31] M. Schecter, D. M. Gangardt, and A. Kamenev, Ann. Phys. (Amsterdam) **327**, 639 (2012); K. Anoshkin, Z. Wu, and E. Zaremba, Phys. Rev. A **88**, 013609 (2013); G. Arwas, A. Vardi, and D. Cohen, Phys. Rev. A **89**, 013601 (2014).

[32] Y. Li, W. Pang, and B. A. Malomed, Phys. Rev. A **86**, 023832 (2012); Y. Li, W. Pang, and B. A. Malomed, in *Localized Excitations in Nonlinear Complex Systems: Current State of the Art and Future Perspectives*, edited by R. Carretero-González *et al.* (Springer, New York, 2014), p. 171.

[33] F. D. M. Haldane, Phys. Rev. Lett. **47**, 1840 (1981).

[34] M. A. Cazalilla, J. Phys. B **37**, S1 (2004).

[35] R. Citro, A. Minguzzi, and F. W. J. Hekking, Phys. Rev. B **79**, 172505 (2009).

[36] Close to the TG limit, a renormalization group calculation yields corrections to the LL result, i.e., an additional reduction of the tunnel energy [37].

[37] D. Yue, L. I. Glazman, and K. A. Matveev, Phys. Rev. B **49**, 1966 (1994).

[38] U. Weiss, Solid State Commun. **100**, 281 (1996).

[39] I. Danshita and A. Polkovnikov, Phys. Rev. B **82**, 094304 (2010); I. Danshita and A. Polkovnikov, Phys. Rev. A **85**, 023638 (2012).

[40] The MPS approach generally performs worse in the weakly interacting regime, where single-particle wave functions are delocalized across the lattice. Moreover the soft-core nature of bosons increases the inaccuracies due to the cutoff in the maximum on-site occupancy (see the Supplemental Material [21]).

[41] A quantitative study for the TG regime has been reported in Ref. [42].

[42] C. Schenke, Ph.D. thesis, Université de Grenoble, 2012, p. 51.

[43] R. Desbuquois, L. Chomaz, T. Yefsah, J. Léonard, J. Beugnon, C. Weitenberg, and J. Dalibard, Nat. Phys. **8**, 645 (2012).

[44] K. K. Das, M. D. Girardeau, and E. M. Wright, Phys. Rev. Lett. **89**, 170404 (2002); P. Vignolo and A. Minguzzi, Phys. Rev. Lett. **110**, 020403 (2013).

[45] A nonmonotonic behavior of tunnel current was also found in fermionic systems in the BCS-BEC crossover [46].

[46] A. Spuntarelli, P. Pieri, and G. C. Strinati, Phys. Rev. Lett. **99**, 040401 (2007).

[47] P.-É. Larré, A. Recati, I. Carusotto, and N. Pavloff, Phys. Rev. A **85**, 013621 (2012).